PHYSICAL REVIEW B VOLUME 38, NUMBER 18 15 DECEMBER 1988-II

Noise spectroscopy of silicon grain boundaries

Armin J. Madenach and Jürgen H. Werner
Max-Planck-Institut für Festkörperforschung, D-7000 Stuttgart 80, Federal Republic of Germany
(Received 6 July 1988)

Noise spectroscopy is a sensitive and versatile tool for the investigation of interface states at semiconductor grain boundaries. We apply a transistorlike model to quantitatively explain observed $1/f$ noise by trapping of majority carriers in grain boundary states. Our model accounts explicitly for spatial electrostatic potential fluctuations within the interface plane due to the random spatial distribution of grain boundary defects. Such spatial inhomogeneities generally cause deviations from Lorentzian noise spectra towards $1/f$ behavior; grain boundaries represent a model system for the study of such a transition. We obtain from our quantitative analysis the density of interface states, their capture cross section, and the standard deviation of the spatial potential fluctuations. Our analysis enables us to derive these three characteristic grain boundary parameters for bicrystals as well as for multicrystalline samples.

I. INTRODUCTION

Electrical fluctuations in physical systems often display a $1/f$ behavior in the dependence of their noise spectra on frequency f.[1] Despite much effort there is still no commonly accepted model for this so-called $1/f$ noise. In the controversy about the physical mechanisms underlying $1/f$ noise, two main approaches can be discerned: One recent approach involves the emission "infraquanta" in the scattering of charged current carriers.[2] This so-called *quantum* $1/f$ model explains Hooge's empirical α-noise model,[1] which assumes mobility fluctuations as the origin for the observed fluctuation phenomena. The physical relevance of Handel's theory[2] and even its derivation are, however, a matter of controversial discussions.[3] Without an underlying microscopic basis, Hooge's model[1] remains, still empirical; no physical parameters can be extracted from measurements with the help of Hooge's model.

Another approach was first discussed by McWhorter[4] for the description of fluctuation phenomena at metal-oxide-semiconductor (MOS) interfaces. McWhorter explained $(1/f)$-like noise by a distribution of time constants τ for capture and emission processes of free-charge carriers.[4] Even though McWhorter's model takes into account the basic physical mechanism underlying the fluctuation processes at MOS interfaces,[5] there remains an arbitrariness in the choice of the proper distribution of time constants. This arbitrariness so far precluded noise measurements from being used as a spectroscopic tool for the quantitative investigation of electronic properties of semiconductor interfaces.

So far, nearly all papers on $1/f$ noise restricted their discussion on spatially homogeneous crystals or, in the case of interfaces, to a perfect order within the boundary plane. For *real* physical systems, however, this (often even tacitly) assumed homogeneity turns out to be an inadmissible simplification. Spatial *inhomogeneities* at semiconductor interfaces necessarily affect their electrical properties and appear to be of paramount importance. Such inhomogeneities were first discussed by Nicollian and Goetzberger;[6] their classic paper[6] about the ac properties of MOS interfaces demonstrated that the random spatial distribution of fixed charges within the oxide results in potential fluctuations within the interface plane. These electrostatic fluctuations at the MOS interface entail a distribution of time constants for the capture and emission of free carriers in interface states. The model of Nicollian and Goetzberger explained ac admittances[6] of MOS interfaces; a first attempt[7] to explain also *noise* with this model was to the best of our knowledge not systematically extended because of a lack of sufficient experimental data as a basis for a quantitative analysis.

The idea of potential fluctuations was recently extended by us to model the ac admittances of current-carrying silicon grain boundaries.[8] Such a potential fluctuations model for *grain boundaries* is based on the fundamental insight that already the localization of carriers in interface states per se (without any fixed charges) leads to a distribution of time constants: The random spatial distribution of charged interface states alone must already result in a spatial modulation of the band edges by electrostatic forces. The resulting *spatial* distribution of time constants explained the frequency dependence of ac admittances of bicrystal grain boundaries.[8] In addition to these results for ac admittances[8] we were indeed also able to interpret $(1/f)$-like noise in the spirit of the earlier[6,7] model of potential fluctuations.[9] The success of our approach was possible because we accomplished a quantitative noise-specific formulation of this model for current-carrying interfaces. The cornerstone of our quantitative analysis was laid with the development of our so-called trap-transistor model for interface states at grain boundaries.[8,9]

Semiconductor grain boundaries are a model system for the investigation of interface states at semiconductor junctions. The electronic properties of the particular "junction" grain boundary are *exclusively* determined by interface traps and their energetic and spatial distribution.[8] These states control the electronic transport prop-

 ©1988 The American Physical Society

erties of polycrystalline semiconductors.[10] Silicon grain boundaries are especially important in semiconductor technology: Fine-grained polycrystalline films[11] in microelectronic circuits as well as coarse-grained solar cells[12] from cast silicon, all suffer from the electronic defects at the junction grain boundary.

The present paper reports in detail how measurements of electrical noise are analyzed to characterize interface states and potential fluctuations at silicon grain boundaries and yield thus essential information about the technologically important polycrystalline silicon. We demonstrate here that the spatial distribution of electronic states within the boundary plane results in particular in a transition from Lorentzian to $(1/f)$-like noise. This noise is experimentally easily accessible due to an inherent amplification mechanism which we term *trap-transistor action.* With the mathematical formulation of our transistorlike model, noise is analyzeable to yield quantitative information about the energetic and spatial distribution of grain boundary defects.

Section II of the present paper describes the sample preparation, and Sec. III portrays our experimental setup. Our trap-transistor model for time-dependent current transport across grain boundaries is sketched in Sec. IV. Section V introduces concepts which are appropriate to account for noise by monoenergetic and continuous energy distributions of interface states. Section VI discusses inhomogeneous charge distribution and describes the evaluation scheme of noise spectroscopy at grain boundaries. Finally, in Secs. VII and VIII we present results for the energy distribution of interface states that were gained by the analysis of noise measurements at artificially grown silicon bicrystals and multicrystals for solar cells.

II. SAMPLE PREPARATION

The systematic investigation of the electric properties of semiconductor grain boundaries requires the examination of boundaries in intentionally grown bicrystals as well as in technologically important multicrystals. Our silicon bicrystals are Czochralski grown by a double seed technique.[13] The geometrical orientation of the two seeds can be deliberately varied. Bicrystal samples discussed in the present paper contain so-called tilt boundaries which grow when two grains are tilted around a common crystallographic axis. All our bicrystals are boron doped with a concentration ranging from 1×10^{14} to 1×10^{16} cm^{-3}. Dopants other than boron are known[14] to segregate at grain boundaries and are thus avoided in the present investigation. The temperature-dependent bulk carrier concentration is determined by Hall measurements within the single crystalline grains. Our samples for the noise measurements are cut perpendicular to the grain boundary. Ohmic contacts are configured as schematically shown in Fig. 1; they are prepared by evaporating aluminum and a subsequent annealing at 500 °C.

Our multicrystals are prepared from commercially available cast polysilicon (Silso by Wacker-Heliotronic) that is also boron doped with a concentration of 3×10^{15} cm^{-3}. The mean diameter of the grains in the investigated multicrystals is about 0.5 mm.

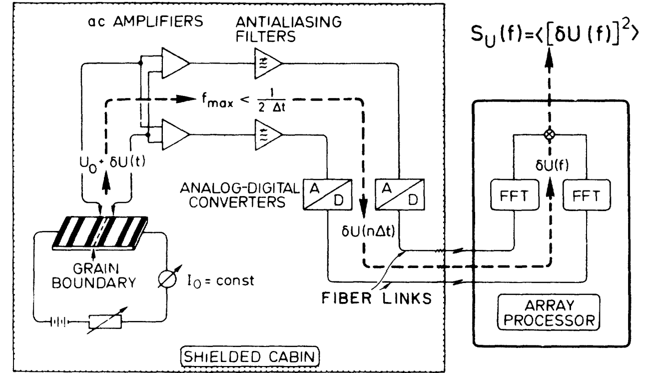

FIG. 1. Experimental setup and contact configuration for measurements at a bicrystal sample. Dashed line indicates how noise voltage $\delta U(t)$ is amplified, filtered, digitized, and transmitted via optical fiber links to the array processor. Signal is split into two branches to enable separate fast Fourier transformation (FFT) and cross correlation which averages out interfering amplifier noise. All devices in the shielded cabin are battery operated.

III. EXPERIMENTAL SETUP

Figure 1 shows a schematic drawing of our setup. We perform our noise measurements by forcing a *constant* current I_0 across the grain boundary. This constant current can be adjusted between 1 nA and 10 mA and is supplied by a bank of batteries in series with a switchable array of metal film resistors. The current I_0 across the grain boundary leads to a voltage drop $U_0+\delta U(t)$ where U_0 denotes the mean value and $\delta U(t)$ the fluctuating noise voltage. The samples are mounted in a cryostat which enables measurements at temperatures between 4 and 500 K.

The noise voltage $\delta U(t)$ is first split into two independent parallel branches of the circuit. Then we amplify (Brookdeal 5004 preamplifiers, Kemo 976 main amplifiers) and filter (Kemo VBF123 antialiasing filters) the signal. Subsequently, we perform a digitization of the signal by homemade analog-to-digital converters (ADC) (maximum clock rate 350 kHz, 12-bit resolution). The cutoff frequency f_{max} of the antialiasing filters is smaller than half the sampling rate of the ADC. The digitized signal is transmitted via optical fiber links to an array processor (floating point systems, AP 120B) where a fast Fourier transform (FFT) is performed. The cross correlation of the two independent branches averages out interfering amplifier noise. Shielding of the whole setup within a Faraday cabin and battery powering of all instruments within the cabin effectively avoids external disturbances.

Very accurate noise spectra which result from many averaging procedures over individual spectra and which have a high resolution on the frequency axis are obtained by us with the help of the considerable computing speed of 12 MFLOPS (million floating-point operations per second) of the array processor. This computing speed enables us to obtain individual noise spectra with 1024 points on the frequency axis in real time up to 30 kHz.

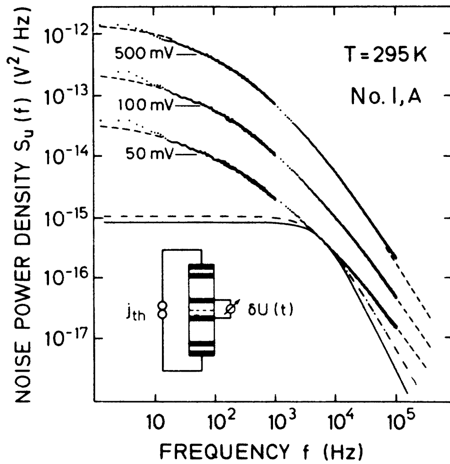

FIG. 2. Noise spectra of a silicon bicrystal for three different voltage drops; shot noise is subtracted. Solid line indicates Lorentzian noise according to Eq. (21) for monoenergetic interface states. Dash-dotted line is for an interface-state continuum after Eq. (22). The dashed lines originate from the potential fluctuations model, Eq. (23), under the consideration of the spatial distribution of interface defects.

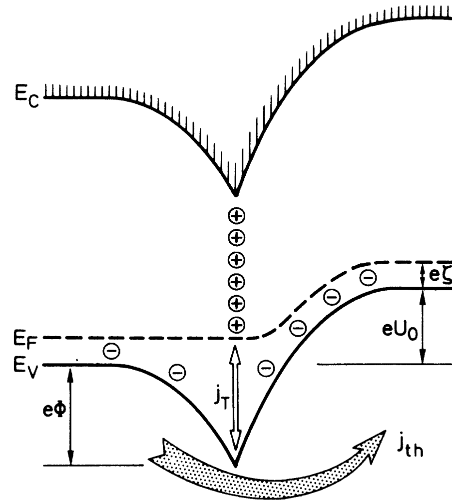

FIG. 3. One-dimensional band diagram at the grain boundary. Only donorlike interface states are drawn for simplicity. The positive interface charge is compensated by negative acceptor ions within the space-charge region. The application of a voltage U results in a thermally emitted current j_{th} over the barrier $e\Phi$. The current j_T represents the capture and emission of holes by the interface states.

Thus, all noise spectra with the exception of the high-frequency spectra above 30 kHz are gained in the same time that is required to sample the signal in the time domain. The required averaging procedure over individual noise spectra is therefore achieved in a reasonable time, thus yielding a small scatter of data points while still maintaining a high resolution on the frequency axis. Our standard measuring routine covers the frequency range from 1 to 100 kHz with 2048 points on the frequency axis. Figure 2 shows typical noise spectra obtained with our setup from a single bicrystal grain boundary with an area of 10^{-2} cm^2. These spectra are in the following analyzed with the combined model of the trap-transistor action and the potential fluctuations.

IV. TRAP-TRANSISTOR MODEL

The crystallographic misfit at the interface plane between two misoriented semiconducting crystallites leads in many cases to electrically charged defect states at the boundary between the grains. This interface charge of areal density Q has in silicon the same polarity as the majority carriers,[8] i.e., a positive interface charge prevails in our p-type samples. The charge Q leads therefore to a potential barrier of height ϕ for the holes, as shown in Fig. 3 in a one-dimensional band diagram.

Free carriers are removed from the depletion regions around the interface. Overall charge neutrality requires the positive interface charge Q to be compensated by the total areal charge Q_R+Q_L of the negative acceptor ions within the depletion regions at the right- and at the left-hand side of the boundary

$$Q=Q_L+Q_R \ . \tag{1}$$

The barrier height Φ can be calculated from the interface charge Q and the depletion charges Q_L, Q_R:[8]

$$e\Phi=\frac{e^2}{2\epsilon\epsilon_0}\frac{Q_L^2}{N}=\frac{e^2}{2\epsilon\epsilon_0}\frac{Q_R^2}{N}-eU_0 \ . \tag{2}$$

Here, N is the doping density, $\epsilon\epsilon_0$ the permitivity of silicon, e the elementary charge, and U_0 the voltage drop across the barrier.

The charge neutrality condition Eq. (1) can be reformulated in terms of the barrier height Φ, which we obtain from the solution of the Poisson equation, Eq. (2):

$$Q=2(C_\Sigma\Phi+C_R U_0) \ . \tag{1a}$$

Equation (1a) introduces the areal geometrical capacitances of the depletion regions, C_R being the capacitance of the right-hand side depletion region

$$C_R=[eN/2\epsilon\epsilon_0(\Phi+U_0)]^{1/2} \ , \tag{3}$$

and C_Σ being the sum of the capacitances of the left-hand side and right-hand side depletion regions

$$C_\Sigma=C_L+C_R=(eN/2\epsilon\epsilon_0\Phi)^{1/2}+C_R \ . \tag{4}$$

The presence of a potential barrier of height Φ leads to a decrease of the conductivity of the polycrystal for the current across the grain boundary. The density j_{th} of this current is usually described by the model of thermionic emission:[15]

$$j_{th}=A^*T^2\exp[-e(\zeta+\Phi)/kT][1-\exp(-eU_0/kT)] \ , \tag{5}$$

where A^* is the effective Richardson constant, kT/e the thermal voltage, and $e\zeta$ the Fermi level within the single crystalline grains. Equation (5) gives the density of the current $I_0 = j_{th} A$ across the boundary with the area A. This current I_0 is kept constant during the experiment. The noise signal which is analyzed consists of the voltage fluctuations δU around the mean voltage drop U_0 which is necessary to maintain I_0.

The measured voltage fluctuations δU are the result of random capture and emission processes of holes at grain boundary interface states. This stochastic trapping of free carriers results in fluctuations δQ of the instantaneous interface charge Q. The interface charge Q determines, however, the barrier height Φ. The charge fluctuations δQ thus lead to fluctuations $\delta\Phi$ in the barrier height Φ which controls the current j_{th} across the boundary as described by the Richardson-Dushman equation for thermionic emission, Eq. (5). In an experiment with a constant *voltage* the barrier fluctuations $\delta\Phi$ could be observed as fluctuations δj_{th} in the over-the-barrier current j_{th}. In our case with a constant *current* source we observe the stochastic fluctuations δU of the corresponding voltage drop U_0.

The stochastic capture and emission of holes at the interface can be described by a fluctuating trapping current j_T, which accounts for the exchange of holes between the valence band and the interface states. In this sense, the current j_T changes the trapped charge Q and thus the band bending Φ and the thermionic hole current j_{th}. The trapping current j_T influences therefore the thermionic current j_{th} via the control of interface charge Q and band bending Φ. This mechanism resembles the current amplification in a bipolar transistor and led us to the name "trap transistor model."[8,9] Similar to bipolar transistor action, very small fluctuations in the modulating trapping current j_T ("base current") are amplified to considerable fluctuations in the emitted current j_{th} ("emitter current") or the corresponding voltage drop U_0.

V. INTERFACE STATE NOISE

A. Noise of monoenergetic centers

The noise power density of the voltage fluctuations δU can be analyzed by considering the fluctuations of the current j_T which changes the interface charge Q. The trapping current j_T is just the time derivation of the charge Q. The time derivation of the interface charge Q is given on the average by the difference of the mean capture and emission rates, R and G, which stand for the areal density of holes being captured and emitted by interface states

$$j_T \equiv e\frac{dQ}{dt} = e(R-G) \ . \tag{6}$$

A phenomenological expression for the mean capture and emission rates, R and G, can be obtained with the help of the Shockley-Read-Hall statistics.[16] If we first consider the particular case of monoenergetic interface states with density N_T located at energy E_T within the forbidden band gap, the two rates are given by[8,16]

$$G = g_p N_T F \ , \tag{7a}$$

$$R = S_p v_{th} N_T (1-F) p_i \ . \tag{7b}$$

Here, S_p denotes the capture cross section of interface states for holes, $v_{th} = (3kT/m^*)^{1/2}$ the thermal velocity of the holes with the effective hole mass m^*, F the occupation of interface states by holes, g_p the emission factor, and p_i is the density of free holes at the interface that is related to the bulk hole density p by

$$p_i = p \exp(-e\Phi/kT) \ . \tag{8}$$

Under steady-state conditions the *mean* value of the trapping current j_T would be zero, i.e., the capture rate would equal the emission rate when we neglect the recombination of electrons and holes at the trapping center. One obtains then from Eqs. (6) and (7) for $R = G$

$$g_p = v_{th} S_p \frac{1-F_0}{F_0} p_i \ , \tag{9}$$

where the subscript zero denotes steady-state values.

So far we considered in Eq. (6) only the dynamics of the *mean* value of the trapping current j_T. Equation (6) does not describe the *instantaneous* value $\tilde{j}_T$ of the trapping current j_T and the corresponding charge fluctuations that lead to the observed noise. A natural way of generalizing a dynamical equation like Eq. (6) to a probabilistic equation for instantaneous quantities as observed in noise experiments is given by the Langevin method:[17] A rapidly fluctuating stochastic force $\xi(t)$ is added to the mean value j_T in Eq. (6) to obtain the instantaneous $\tilde{j}_T$. The force $\xi(t)$ describes the random action of excitations (phonons, photons, etc.) which influence the trapping current j_T at finite temperatures:

$$\tilde{j}_T = j_T + \xi(t) = e(R-G) + \xi(t) \ . \tag{10}$$

The time average of $\xi(t)$ vanishes; the stochastic Eq. (10) complies therefore with Eq. (6) for the mean values. We assume further that the force $\xi(t)$ is uncorrelated on the time scale of our measurements. This assumption means that it is supposed that the value $\xi(t)$ at time t does not dependent on the value $\xi(0)$ at time $t=0$. This requirement should always be fulfilled for our experiments with a maximum frequency of 100 kHz when one imagines that the force $\xi(t)$ represents, for example, phonon processes on a typical time scale of picoseconds. Our assumption is mathematically expressed by requiring that the correlation function $C_\xi(\rho) := \langle \xi(0)\xi(\rho) \rangle$ of the stochastic force $\xi(t)$ is proportional to a δ function $C_\xi(\rho) = c\delta(\rho)$, where c denotes a constant.[17] Equivalently, the frequency-dependent power spectrum $S_\xi(f)$ of the stochastic force $\xi(t)$, which is defined by the Fourier transform of the correlation function $C_\xi(\rho)$, i.e.,[18]

$$S_\xi(f) := 2\int_0^\infty \exp(-2\pi i f \rho) C_\xi(\rho) d\rho = 2\langle |\xi(f)|^2 \rangle = c \tag{11}$$

becomes independent of frequency f and equal to the constant c. The factor c is discussed below.

We may now calculate the power spectrum $S_Q(f)$ of the interface charge fluctuations δQ. In a first step, we linearize the instantaneous trapping current $\tilde{j}_T(t)$, Eq. (10), around its mean value $j_{T0}(t)$ and obtain for the fluctuations $\delta j_T(t)$ around the mean values

$$\delta j_T(t)=\frac{d}{dt}\delta Q(t)=S_p v_{\rm th}\left[N_T(1-F_0)\delta p_i(t)-\frac{p_{i0}}{F_0}\delta Q(t)\right]+\xi(t)\ . \quad (12)$$

We next perform a Fourier transform of Eq. (12) into the frequency domain and eliminate the Fourier coefficients $\delta p_i(f)$ with the help of Eqs. (1a) and (5). Thus, we are able to determine the Fourier coefficients $\delta Q(f)$ of the charge fluctuations $\delta Q(t)$:

$$\delta Q(f)=\frac{\tau\xi(f)}{1+i2\pi f\tau} \quad (13)$$

with the time constant τ defined by

$$\tau^{-1}=\frac{v_{\rm th}S_p p_{i0}}{F_0}\times\left[\frac{e^2N_TF_0(1-F_0)}{kT\{C_\Sigma+C_R[\exp(eU_0/kT)-1]\}}+1\right]\ . \quad (14)$$

In Eqs. (13) and (14) we take explicitly into account the experimental condition of a constant over the barrier current $j_{\rm th}$. The *noise spectrum* $S_Q(f)$ of the *charge fluctuations* $\delta Q(t)$ is obtained from the square $\langle|\delta Q(f)|^2\rangle$ according to the definition of the spectrum in Eq. (11) but now applied to the charge fluctuations $\delta Q(f)$:

$$S_Q(f)=\frac{\tau^2 S_\xi}{1+(2\pi f\tau)^2}\ . \quad (15)$$

The spectrum S_ξ of the stochastic force ξ is independent of frequency f and equal to the constant c; the frequency dependence of the spectrum $S_Q(f)$ of charge fluctuations is therefore given by the frequency dependence of the denominator in Eq. (15). Therefore, we can easily determine the standard deviation $\langle\delta Q^2(t=0)\rangle$ by integrating the noise spectrum $S_Q(f)$ over all frequencies, as follows immediately from the inverse Fourier transform, Eq. (11), which relates the correlation function with its spectral density:

$$\langle\delta Q^2(t=0)\rangle=\tfrac{1}{2}\int_0^\infty S_Q(f)df=S_\xi\tau/4=c\tau/4\ . \quad (16)$$

The standard deviation, was calculated by van Vliet and Fassett.[19] Using their Eq. (57), we obtain

$$S_\xi=4S_p v_{\rm th}p_{i0}N_T(1-F_0)/A\ . \quad (17)$$

Combining Eqs. (15) and (17), we derive the final result for the spectrum of the charge fluctuations

$$S_Q(f)=\frac{4\tau^2 v_{\rm th}S_p p_{i0}N_T(1-F_0)}{A[1+(2\pi f\tau)^2]}\ . \quad (18)$$

The spectrum $S_U(f)$ of the corresponding *voltage fluctuations* $\delta U(t)$ results from our trap-transistor action. The relation between the charge fluctuations δQ and the corresponding voltage fluctuations δU can be determined quantitatively with the help of the charge neutrality condition Eq. (1) and the transport current $j_{\rm th}$ from Eq. (5):

$$\delta U/\delta Q=\frac{e[\exp(eU_0/kT)-1]}{C_\Sigma+C_R[\exp(eU_0/kT)-1]}\ . \quad (19)$$

We obtain then for the spectrum $S_U(f)$ of voltage fluctuations of grain boundaries containing monoenergetic traps:

$$S_U(f)=(\delta U/\delta Q)^2S_Q(f)\ . \quad (20)$$

Since our experiments are carried out under the condition $eU_0\gg kT$, relations (14) and (19) can be simplified as follows:

$$S_U^{\rm mono}(f)=\alpha_{\rm mono}N_T(1-F_0)\frac{\tau_{\rm mono}^2}{1+(2\pi f\tau_{\rm mono})^2}\ , \quad (21a)$$

$$\alpha_{\rm mono}=\frac{4e^2p_{i0}v_{\rm th}S_p}{AC_R^2}\ , \quad (21b)$$

$$\tau_{\rm mono}=F_0(v_{\rm th}S_p p_{i0})^{-1}\ . \quad (21c)$$

Equation (21a) predicts a Lorentzian curve for the frequency dependent noise of monoenergetic interface states: The noise displays a low-frequency saturation value $S_U^{\rm mono}(f\to 0)=\alpha_{\rm mono}N_T(1-F_0)\tau_{\rm mono}^2$ and a decay with $1/f^2$ at high frequencies. A comparison of measured noise $S_U(f)$ with Eq. (21a) is most conveniently achieved in a plot of $2\pi f S_U(f)$ versus frequency f. Equation (21a) predicts for such a Lorentz curve a maximum of height $\alpha_{\rm mono}N_T(1-F_0)\ \tau_{\rm mono}^2/2$ at a frequency $f=f_{\max}$ where $2\pi f\tau_{\rm mono}=1$ holds. The frequency and the height of the maximum yield therefore the time constant $\tau_{\rm mono}$ as well as the prefactor of Eq. (21a).

Figure 2 shows a comparison of measured bicrystal noise with Eq. (21a). The calculated solid line in Fig. 2 deviates considerably from the measured data. The experimental results are therefore not satisfactorily explainable with a noise model of monoenergetic interface states.

B. Noise of energy continua

Grain boundaries are the location of distorted and broken bonds, impurities, and primary and secondary dislocations which originate from the accommodation of the crystallographic misfit between the two grains.[8,10] It seems unlikely that these potential charge sites are equally and so regularly configured in the lattice that just monoenergetic centers arise within the forbidden gap. Instead, it seems more probable that such levels are continuously distributed over energy. A more realistic model of noise due to capture and/or emission of free carriers in interface states considers therefore a continuous density of states $N_{SS}(E)$.

Noise due to capture processes into continuously distributed states can generally not be exactly calculated. Lee *et al.*[20] demonstrated, however, that such noise spectra can be approximated by an integration of Lorentz spectra over energy E if the number of charged trap

states is much smaller than the number of free carriers which are available for capture. We use this approximation and integrate Eq. (21) over energy. This integration is conveniently achieved by transforming the integration over energy in an integration over occupation F_0 which yields finally

$$S_U^{\text{cont}}(f)=\alpha_{\text{cont}}\frac{N_{SS}}{(2\pi f)^2\tau_p}\ln[1+(2\pi f\tau_p)^2] \;, \tag{22a}$$

$$\alpha_{\text{cont}}=\frac{2kTe^2}{AC_R^2} \;, \tag{22b}$$

$$\tau_p=(v_{\text{th}}S_p p_{i0})^{-1} \;. \tag{22c}$$

Comparison of measured noise $S_U(f)$ with the model for continua, Eq. (22a), is also obtainable from a plot of $2\pi f S_U(f)$ versus frequency f. A maximum of height $0.4\alpha_{\text{cont}}N_{SS}\tau_p$ at frequency $f=f_{\text{max}}$ occurs, where $2\pi f_{\text{max}}\tau_p=1.98$ holds. Height and frequency of the maximum yield therefore density of states N_{SS} and time constant τ_p.[9]

The spectral density $S_U^{\text{const}}(f)$ of Eq. (22a) is represented by the dash-dotted line in Fig. 2. Evidently, a continuous energy distribution of interface states alone is also insufficient to explain the measured data. In fact, the frequency dependent $S_U^{\text{cont}}(f)$ differs only slightly from the Lorentzian behavior $S_U^{\text{mono}}(f)$ after Eq. (21a) since only states around the steady-state Fermi level contribute to the noise.[20]

VI. POTENTIAL FLUCTUATIONS

The discrepancy between the Lorentzian form of Eq. (21) or its modification, Eq. (22), and the measured spectra is a result of an inadmissible simplification which is inherent to the *one-dimensionality* of the model discussed in Sec. V: Our discussion assumed tacitly thus far that the grain boundary is electrically homogeneous. The boundary is, however, not homogeneously charged like a metallic disk. Instead, the charges in the trap states stem from localized carriers with typical interdistances of 10–100 nm. The spatial distribution of the charge sites within the grain boundary must therefore necessarily result in a spatial modulation of the band bending at the interface. In an earlier publication[21] we were, for example, able to correlate such electrical inhomogeneities with the spatial distribution of secondary dislocations which were analyzed by structural analysis and admittance spectroscopy.[8]

Consideration of the interfacial potential fluctuations leads also to a modification of our one-dimensional noise model of Sec. V. Figure 4 shows the spatial distribution of positive interface charges with the resultant modulation of the band edges in a band diagram which is projected onto the interface plane. Such fluctuations have a drastic impact on the noise properties of the grain boundary because they dramatically influence the capture time constant: Equation (22c) reveals that the time constant τ_p depends linearly on the steady-state hole concentration p_{i0} at the grain boundary which, according to Eq. (8), depends *exponentially* on barrier Φ. The modulations of the barrier Φ yield thus drastic spatial fluctuations of the time constants τ_p and a considerably different noise behavior. The consideration of the inhomogeneous potentials allows us to explain the measured noise quantitatively.

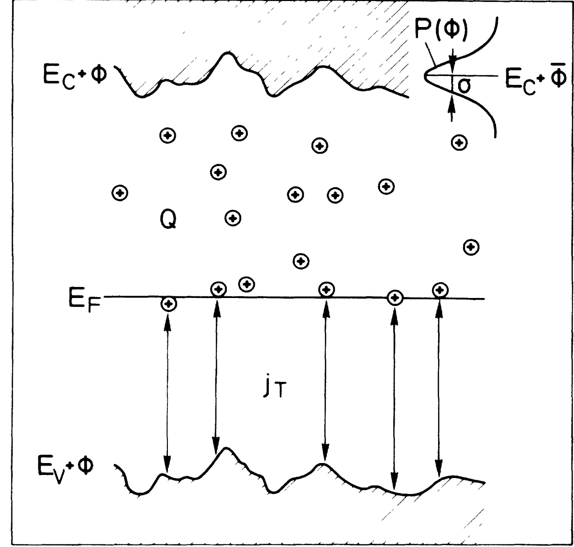

FIG. 4. Band diagram as projected onto the interface plane. The random spatial distribution of trapped positive interface charges leads to an electrostatic modulation of the band edges along the interface. These potential fluctuations are modeled by a Gaussian distribution $P(\Phi)$ around a mean barrier height $\overline{\Phi}$ with standard deviation σ.

The distribution $P(\Phi)$ of barrier heights Φ is in a first approximation a Gaussian distribution with mean barrier height $\overline{\Phi}$ and standard deviation σ:

$$P(\Phi)=\frac{1}{(2\pi\sigma)^{1/2}}\exp\left[\frac{(\Phi-\overline{\Phi})^2}{2\sigma^2}\right] \;. \tag{23a}$$

We consider the contribution to the noise spectrum due to capture and emission of charge carriers which traverse the boundary at different barrier heights Φ as independent. The total noise spectrum is then obtained by integrating over all noise contributions. Each contribution has to be weighted by probability $P(\Phi)$, and we integrate over deviations $\Phi-\overline{\Phi}$:

$$S_U^{PF}:=\int_{-\infty}^{+\infty}P(\Phi)S_U^{\text{cont}}(f)d(\Phi-\overline{\Phi}) \;. \tag{23b}$$

The resulting spectral density, S_U^{PF}, is now in excellent agreement with the measurements as also demonstrated in Fig. 2.

The evaluation of the measured spectra on the basis of this potential fluctuations model cannot be performed analytically. We are thus forced to make use of a numerical evaluation procedure that is similar to one which was first proposed by Simonne[22] and then extended by Werner[8] for the evaluation of admittance spectra: We multiply the measured noise $S_U(f)$ with the angular fre-

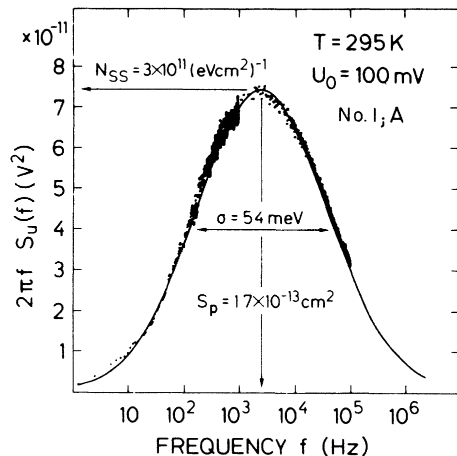

FIG. 5. The product of measured noise $S_U(f)$ and frequency $2\pi f$ for the 100-mV spectrum of Fig. 2. Solid line is obtained from the potential fluctuation model Eq. (23) with the shown values for density of states N_{SS}, capture cross section S_p, and standard deviation σ of the spatial potential fluctuations.

quency $2\pi f$. This product, $2\pi f S_U(f)$, shows a broad maximum as demonstrated in Fig. 5 for the 100-mV data of Fig. 2. From the height of this maximum we obtain the density of interface states N_{SS}; the position of the maximum yields the mean constant τ_p and the hole capture cross section S_p; the width of the curve is a measure for the standard deviation σ of the spatial potential fluctuations.

We use only the data point at the maximum of curves like the one in Fig. 5 and one additional point of the curve to determine the three parameters N_{SS}, S_p, and σ. Then we integrate Eq. (23) and compare with the complete set of the frequency-dependent data as shown in Fig. 2 where the integrated data are represented by the dashed line. The agreement over a frequency range of five decades supports the validity of our model. Moreover, we already demonstrated earlier that the results from our noise spectroscopy agree well with those from admittance spectroscopy.[9]

Our model as here discussed enables us to quantitatively evaluate noise spectra of silicon grain boundaries. By variation of temperature T and/or of the voltage drop U_0 we sweep the stationary Fermi level $E_F = e\zeta - e\Phi$ through the forbidden gap. We are thus able to investigate the energy dependence of the density of states N_{SS} and the capture cross section S_p. We further obtain the standard deviation σ, thus quantitative information, about interfacial inhomogeneities.

VII. RESULTS FOR BICRYSTALS

A. Density of states N_{SS}

In a detailed study we analyze the energy dependence of N_{SS} at two different bicrystals. Both bicrystals with the specimen numbers 1 and 2 are boron doped with a concentration of 9×10^{14} and 3×10^{15} cm^{-3}, respectively. Both samples contain a $\langle 110 \rangle$-tilt boundary; the tilt angles being 8° and 10°, respectively. The density of states N_{SS} is analyzed by several independent methods; the comparison allows us to check the correctness of results obtained by noise spectroscopy.

Figure 6(a) compares results for the density of states at the grain boundary of sample A cut from bicrystal no. 1. The data stem from three different methods: Noise spectroscopy, admittance spectroscopy,[8] and from current voltage curves.[9,15] Good agreement between the results of these three methods is observed. The high value for the density of states at midgap pins the dark Fermi level within this energy range. Our earlier measurements[23] of photocapacitance of a different sample B from the same bicrystal reveal the density of states over a wider energy range, as shown in Fig. 6(b). In particular, we find at the conduction-band edge a band tail which can be fitted by an exponential decay:

$$N_{SS}^C(E) = N_0^C \exp(-\Delta E / E_0^C) \tag{24}$$

with $N_0^C = 9\times10^{14}$ eV^{-1}cm^{-2} and $E_0^C = 11$ meV. Here ΔE denotes the energy distance measured from the conduction-band edge.

Band tails at the grain boundary are expected as a consequence of the spatial disorder on a length scale of a few lattice constants.[24] The finding of band tails in the density of states corroborates therefore our model of spatial inhomogeneities. Band tailing states result from carrier localization in local potential maxima and minima of the valence- and conductance-band edges. Tail states in spatially disordered systems and their connection with the spatial distribution of localized charges are well known in amorphous semiconductors and were discussed by Cohen, Fritsche, and Ovshinsky.[25] The relevance of band tails and a model for their occurrence in polycrystalline semiconductors was recently pointed out by Werner and Peisl.[26]

Another example for band tails at silicon grain boundaries is shown in Fig. 6(c) which presents results from noise measurements and I-V curves at a sample from bicrystal 2. In this sample we are able to investigate a wide energy range by variation of temperature and bias because no additional midgap states pin the Fermi level. We find an exponential tail with a drop of almost four decades within 0.3 eV. The tail can be fitted by

$$N_{SS}^V(E) = N_0^V \exp(-\Delta E / E_0^V) \tag{25}$$

with $N_0^V = 6\times10^{14}$ eV^{-1}cm^{-2} and $E_0^V = 30$ meV where ΔE denotes the energy distance to the valence-band edge.

The values N_0^C and N_0^V are obtained from two different samples and stand for the density of states when one extrapolates the measured data towards the band edges. It is therefore interesting to note that the experimental N_0^C, N_0^V values are close to the theoretical values which one expects for two-dimensional gases of *free* electrons and holes in the conduction band and valence band, respectively. These theoretical data are calculated similar to the values of Werner and Peisl[26] and are indicated by the arrows at the band edges in Figs. 6(b) and 6(c). Here we follow an universal model of Soukoulis, Cohen, and Economou[27] who discussed the general relationship between the slopes and band-edge values of exponential

tails in disordered systems.

Figure 6(b) presents a compilation of results for sample *B* from bicrystal no. 1 which were obtained by different techniques: The equilibrium Fermi level is located at $E \approx 0.5$ eV and the data at energies $E \leq 0.5$ eV stem from the evaluation of temperature-dependent noise spectroscopy, admittance spectroscopy, and current-voltage curves. The results for $E \geq 0.5$ eV were earlier measured by us by photoconductance and photocapacitance.[8,23] It is interesting to note that the density of states at this grain boundary drops indeed sharply around 0.5 eV as already earlier concluded on basis of the results from photocapacitance.[8,23] The results of noise, admittance spectroscopy, and *I-V* curves confirm this finding and reveal a value of up to $N_{SS} = 4 \times 10^{12}$ cm^{-2}eV^{-1} around 0.3 eV. The high N_{SS} value in this energy range prevents the Fermi level from moving closer to the valence-band edge. It is therefore impossible to analyze the valence-band tail in bicrystal no. 1. The dashed line at the valence-band edge depicts the tail that—according to Fig. 6(c)—we expect to measure if we were able to shift the Fermi level up to this energy.

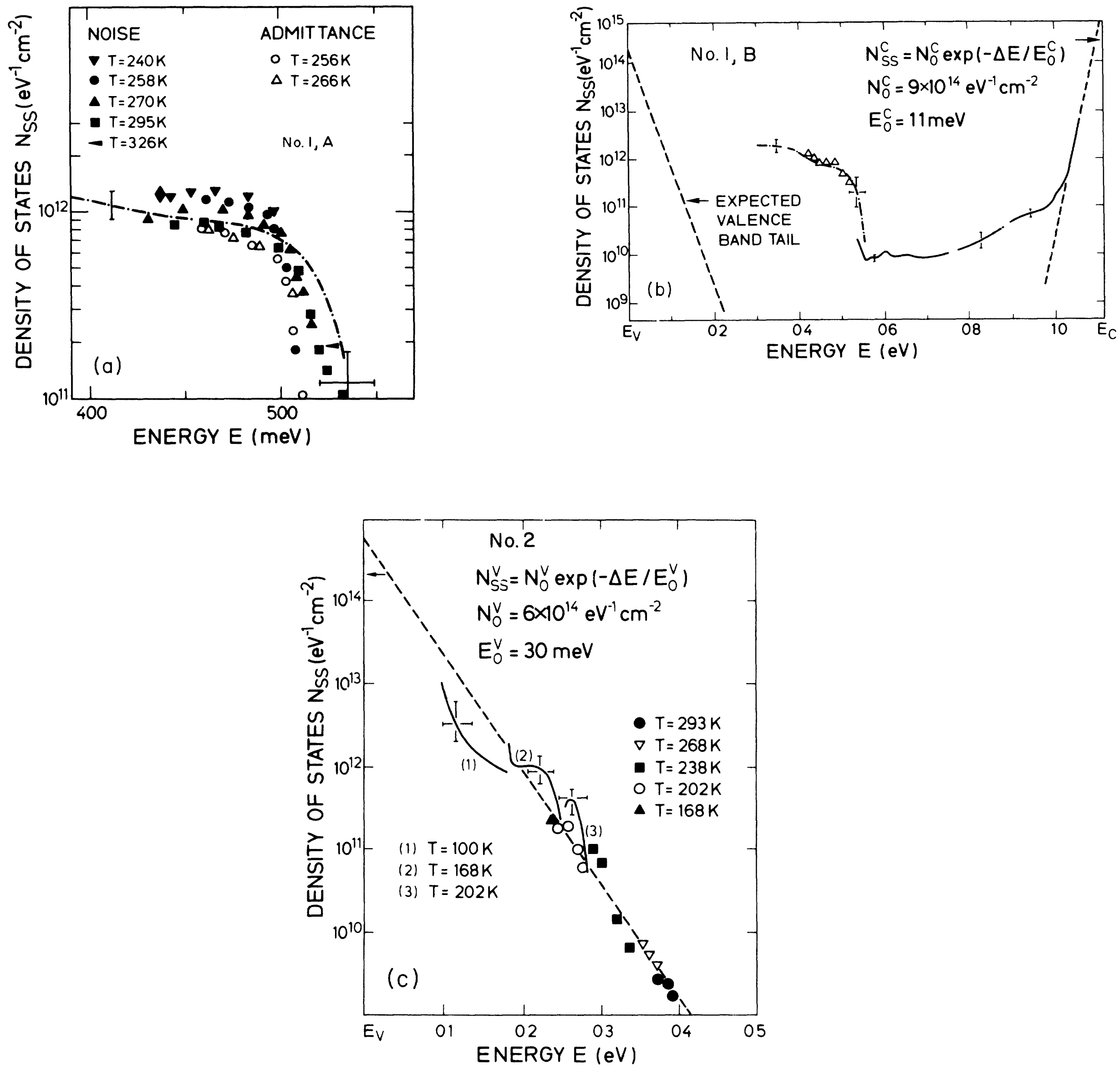

FIG. 6. (a) Density of interface states N_{SS} of sample *A* from bicrystal no. 1 as determined by noise spectroscopy (solid symbols), admittance spectroscopy (open symbols), and *I-V* measurements (dash-dotted line). The zero point of the energy axis lies at the valence-band edge. (b) Density of states of sample *B* from bicrystal no. 1 as determined by noise spectroscopy (triangles), *I-V* measurements (dash-dotted line), and photocapacitances (solid lines). At the conduction-band edge, an exponential band tail is found. The expected valence-band tail is covered by a high density of midgap states. (c) Density of interface states of a sample from bicrystal no. 2 as determined by noise spectroscopy (symbols) and *I-V* measurements (solid lines).

B. Capture cross section

The evaluation of the noise at the maxima in curves such as Fig. 5 yields the time constant τ_p and then from Eq. (22c) the capture cross section S_p of the interface states. From the analysis of experiments at bicrystal no. 1, we find capture cross sections S_p around 10^{-13} cm^2. There are again two possibilities to examine the energy dependence of S_p: Variation of bias voltage and variation of temperature. In both cases the stationary Fermi level is shifted through the forbidden gap. When we analyze the energy dependence of S_p by varying the bias voltage at a fixed temperature we obtain an apparent strong dependence of S_p on energy. However, when we scan the same energy regime by varying the temperature at a fixed bias voltage this seemingly energy dependence of S_p cannot be confirmed. In fact, we learn that the apparent energy dependence of S_p is induced by the applied voltage.

Figure 7 demonstrates the dramatic dependence of the capture cross section S_p on the applied bias U_0 which is normalized to the thermal voltage kT. A decrease of S_p by almost 2 orders of magnitude is observable. Such surprising dependences are unknown from traps in the bulk of homogeneous semiconductors[28] as well as from traps in MOS transistors.[6] The observed voltage dependence seems therefore to be related to a fundamental difference between traps at MOS interfaces or in bulk semiconductors and our current carrying grain boundaries.

We do not offer perfect quantitative explanation for the observed behavior but we propose that the observed voltage dependence is caused by the high electric fields at the grain boundary which results in unidirectional net current flow which is accompanied by high carrier velocities: The high speed of the free holes which cross the interface decreases the capture probability and lowers thus the observed capture cross section S_p.

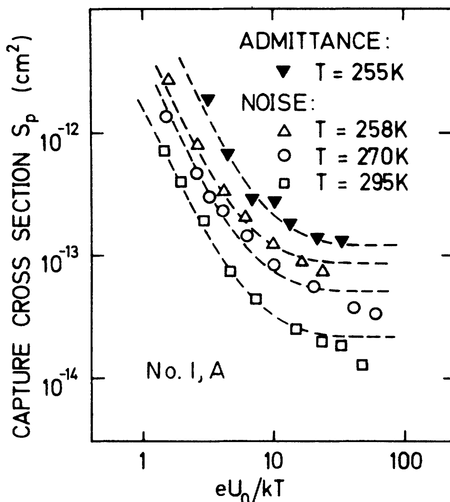

FIG. 7. The capture cross section S_p depends on voltage drop U_0. This finding is explained by a dependence of S_p on the velocity of the carriers which cross the interface (dashed line).

Quantitatively we model the voltage dependence of S_p by analyzing the cross section's dependence on the mean carrier transport velocity v_i of holes across the interface. Spatial constancy of the current at any point x in a one-dimensional model

$$j = ep(x)v(x) \tag{26}$$

and, according to Eq. (8), the low hole concentration p_i at the grain boundary requires that the velocity v_i at the interface is orders-of-magnitude higher than in the bulk. A quantitative expression for v_i is obtained by rewriting the current j_{th} in Eq. (5) with the equality

$$A^*T^2 = eN_c\bar{v}/4 , \tag{27}$$

where $\bar{v} = v_{\text{th}}[8/(3\pi)]^{1/2}$ holds.[29] From a comparison of Eqs. (26) and (27) we thus obtain

$$v_i = (v_{\text{th}}/4)[1-\exp(-eU_0/kT)] . \tag{28}$$

Equation (28) shows that the hole velocity v_i at the interface increases with increasing bias voltage and saturates at $v_{\text{th}}/4$ for $eU_0 \gg kT$.

For Coulombic trapping centers, the capture cross section S_p depends on velocity v according to a power law $S_p \sim v^{4}$.[30] We expect therefore a voltage dependence of S_p according to

$$S_p = S_p^0(T)[1-\exp(-eU_0/\nu kT)]^{-4} . \tag{29}$$

Here, $S_p^0(T)$ is a voltage-independent factor that may still depend on temperature.

The dashed lines in Fig. 7 are calculated with Eq. (29) and demonstrate a reasonable agreement with the measured voltage dependence at various temperatures. However, we have to introduce an "ideality" factor $\nu > 1$ in order to fit Eq. (29) to our experimental results. The physical significance of this ν with a value of $\nu \approx 4$ is not yet understood. This factor may, for example, be a hint to an increased carrier temperature at the interface or, the factor, might indicate a voltage-induced change of the trap occupation by minority carrier injection. The good agreement between measured capture cross sections and the predictions of Eq. (29) gives, however, strong support for our underlying physical idea of a velocity-dependent capture cross section.

C. Standard deviation σ

The third physical quantity obtained by noise spectroscopy at grain boundaries is the standard deviation σ of spatial potential fluctuations. Our experiments yield typical values of $\sigma \approx (2-3)kT$ for the width of the Gaussian potential distribution with a typical mean barrier Φ around 300 meV. The potential fluctuations are the result of the spatial *charge* distribution and σ can therefore also be used to gain information on the charge distribution itself.

For the analysis of σ we use a model of Brews[31] that was originally developed for MOS interfaces. Within this model the measured standard deviation σ is related to the correlation length λ of the spatial charge distribution according to[21,31]

$$\lambda = \frac{\epsilon\epsilon_0}{eC_{\Sigma} + eN_{SS}} \left[\exp\left[\frac{16\pi\epsilon\epsilon_0\sigma^2}{e^2 Q} \right] - 1 \right]^{-1/2} . \quad (30)$$

Figures 8(a) and 8(b) depict the resulting correlation length λ as a function of band-gap energy E. Here the energy values represent the position of the stationary Fermi level which is varied by voltage and temperature. The scatter of the λ values is a result of the sensitive exponential dependence on the experimentally determined standard deviation σ and interface charge Q. In spite of the scatter of the data points, we observe a good agreement between the results from noise and admittance spectroscopy. There is also no significant energy dependence observable. This finding indicates that the change of charge by the application of a bias does not induce a significant change of the spatial distribution of potentials.

In a previous work, Werner and Strunk[21] were able to relate the correlation length λ of our sample no. 1 to secondary dislocations along the boundary. The lines of these secondary dislocations were randomly distributed within an array of regularly spaced primary dislocations. Such secondary dislocations are therefore probable candidates for the location of the randomly spaced interface charges which cause the measured potential fluctuation. The minimum distance of 7 nm between the dislocation lines[8,21] appears to correlate well with the measured correlation length λ as shown in Fig. 8(a).

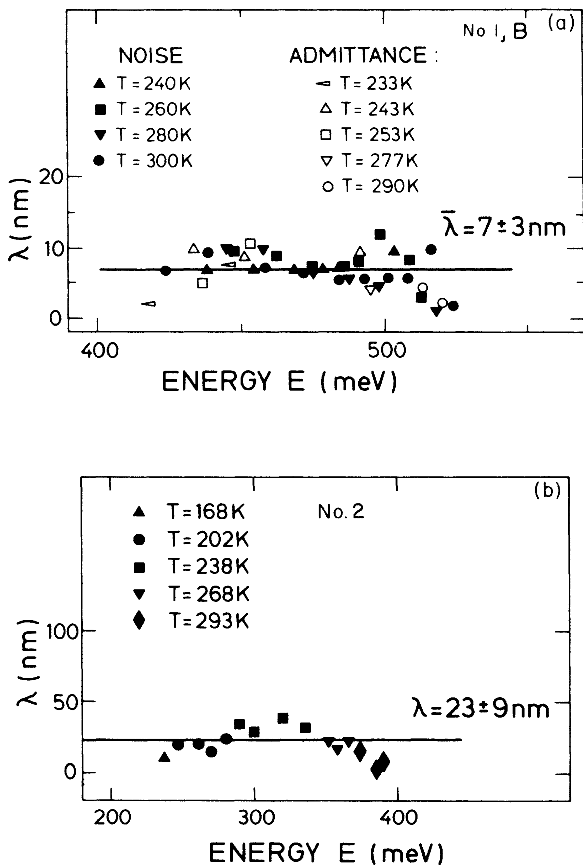

FIG. 8. (a) Correlation length λ of spatial potential fluctuations in sample B from bicrystal no. 1 as determined by noise spectroscopy (solid symbols) and by admittance spectroscopy (open symbols). (b) Correlation length λ in a sample from bicrystal no. 2 as determined by noise spectroscopy. For both samples, the energy zero point lies at the valence-band edge.

VIII. MULTICRYSTALLINE SAMPLES

Grain boundaries in polycrystalline silicon dominate the electronic properties of devices in semiconductor technology as, for example, solar cells[12] or integrated circuits.[11] Characterization methods for polycrystalline silicon should therefore be applicable not only to bicrystals but also to polycrystals containing a multitude of grain boundaries. In the previous sections we demonstrated that noise spectroscopy is a sensitive tool for the analysis of single boundaries in bicrystals. In this section, we show now that the same techniques are also applicable to multicrystals. Here we apply noise spectroscopy to a sample which is cut from a cast p-type multicrystal (Silso) grown by Wacker-Heliotronic for solar cells. The 400 μm thick sample is boron doped with a concentration of $N_A = 3\times10^{15}$ cm^{-3} and has a mean grain size around 500 μm. Most grains are therefore large enough to be extended through the whole thickness of the wafer. The noise spectrum of the sample is shown in Fig. 9.

The theory of the previous paragraphs can be applied to such a multicrystal when we ascribe the noise from the many grain boundaries within the sample to a hypothetical single, *mean* boundary which represents then the average properties of all grain boundaries within the polycrystal. The noise of such a hypothetical mean

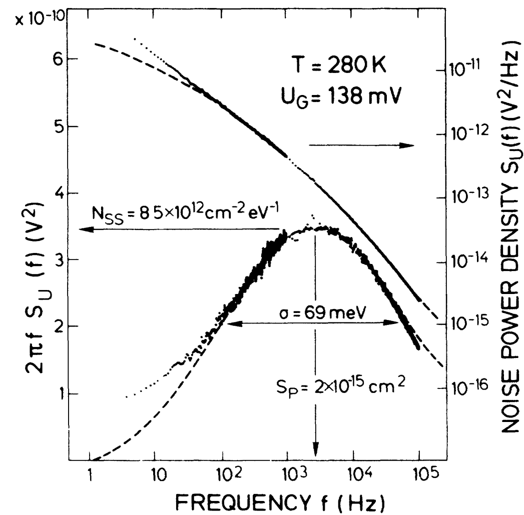

FIG. 9. Noise power density $S_U(f)$ and $2\pi f S_U(f)$ obtained from a multicrystalline sample at a mean voltage drop $U_G \simeq 138$ mV per barrier. The dashed lines result from the potential fluctuations model, Eq. (23), with the shown values for the density of states N_{SS}, the capture cross section S_p, and the standard deviation σ which reflects spatial potential fluctuations as well as variations of the mean barrier height from boundary to boundary.

boundary can then be analyzed with the theory developed in the previous sections.

The noise of such a mean boundary is determined with the help of the following consideration: In a good approximation we may consider a network of grain boundaries to act as an array of independent noise sources. This assumption holds as long as there is no interaction of grain boundaries, for example, by an overlap of the space-charge regions. This situation is always encountered for our coarse-grained polycrystals. The typical width of 1 μm for the space-charge regions is always small compared to the grain size. The polycrystal may then be schematized as shown in Fig. 10.

The multicrystal is represented by an array of cubic, identical grains. The grain boundaries between the grains are assumed to be equal and they have the properties of an averaged, *mean* boundary of the real, irregular sample. There are l grain boundaries with their area perpendicular to the current flow and we count q boundary areas parallel to the main direction of the current. The l grain boundaries in series increase the noise S_G of a single mean boundary by a factor l. Equations (21) and (22) demonstrate that the noise of a single boundary is proportional to the inverse grain boundary area A. The connection of q boundary areas parallel to the current flow leads to an increase in the sample cross section by a factor q and accordingly to a decrease by a factor $1/q$ in the total noise S_U with respect to the noise originating from a mean boundary. We can thus relate the total measured noise S_U of the polycrystal to the noise S_G of a hypothetical mean grain boundary:

$$S_U(f)=\frac{l}{q}S_G(f)\ . \tag{31}$$

The noise power density generated on the average by a single grain boundary, $S_G(f)$, can be analyzed with the help of the model developed in Secs. V and VI. Our potential fluctuations model takes implicitly into account the wide range of barrier heights which differ for the various grain boundaries. The extracted standard deviation σ of the potential fluctuations is therefore no longer a measure for spatial potential fluctuations within a single grain boundary alone. Instead, σ measures also the variation of the mean barrier heights from boundary to boundary. Thus, we expect σ to have larger values for multicrystalline samples than for single boundaries in bicrystals.

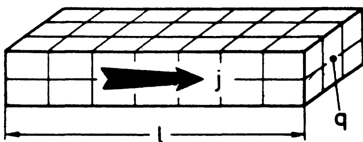

FIG. 10. Simplified model for a polycrystal. The different crystals and their interfaces are replaced by identical, *mean* grains and grain boundaries. Their number perpendicular to current j is $l=6$ and within one row there are $q=6$ boundary areas parallel to j.

The polycrystal's noise in Fig. 9 resembles indeed the noise of a single boundary in Fig. 2. The noise in Fig. 9 indicates, however, a $(1/f)$-like behavior over a wide frequency range, which is a consequence of a larger σ value. We count in the Silso sample $l=13$ grain boundaries perpendicular to the current along a distance of 5.2 mm. The analysis with the help of an optical microscope yields $q=15$ boundary areas on a width of 6 mm between the voltage contacts.

The evaluation of the maximum in Fig. 9 yields a density of states $N_{SS}=8.5\times10^{12}$ eV^{-1}cm^{-2} at an energy $E=370$ meV above the valence-band edge. This N_{SS} value exceeds those observed at our artificially grown bicrystal boundaries. The standard deviation $\sigma=70$ meV is also larger than the data from bicrystals where we found always σ values below 55 meV. The large value of σ for the hypothetical mean grain boundary barrier of the multicrystalline sample is easy to understand: Our hypothetical, averaged, mean grain boundary must represent the spatial modulations within single boundaries as well as the fluctuations from boundary to boundary.

IX. FROM LORENTZIAN TO 1/f NOISE

We now reconsider the general problem of $1/f$ noise in the light of the potential fluctuations model proposed in this work. Figure 2 shows that the presence of an irregular spatial distribution of interface charges leads to a considerable broadening of traditional Lorentzian noise spectra. Depending on the degree of the spatial disorder, which is quantitatively expressed by the standard deviation σ of the spatial potential fluctuations, or its dimensionless equivalent

$$\sigma_T:=e\sigma/kT \tag{32}$$

we observe a continuous broadening of noise spectra. Large values for σ_T yield finally a $1/f$ dependence over a considerable frequency range as shown in Fig. 9 for the multicrystal.

Such a transition from Lorentzian noise towards $1/f$ noise is exemplified in Fig. 11 which compares data from the samples discussed in the present paper. In the various spectra displayed in Fig. 11, the frequency span in which the spectra approach a $1/f$ behavior extends over more than one, two, and about three decades depending on the value of $\sigma_T=1.5$, 2.12, and 2.85, respectively.

The transition from Lorentzian noise to $1/f$ noise can be understood in terms of a distribution function $g(\tau)$ of time constants for capture and emission processes. This distribution function can be calculated if we change the integration variable in Eq. (23) from $\Phi-\overline{\Phi}$ to τ:

$$S_U^{PF}(f)=\int_{-\infty}^{+\infty}P(\Phi)S_U^{\text{cont}}(f)d(\Phi-\overline{\Phi})$$
$$=\int_0^{\infty}S_U^{\text{cont}}(f)g(\tau)d\tau\ . \tag{33}$$

Equation (33) yields then together with Eq. (23a):

$$g(\tau)=\frac{1}{\tau(2\pi\sigma_T)^{1/2}}\exp\left[-\ln^2\left[\frac{\tau/\tau_p}{2\sigma_T^2}\right]\right]\ . \tag{34}$$

Figure 12 shows the distribution function $g(\tau)$ for typical

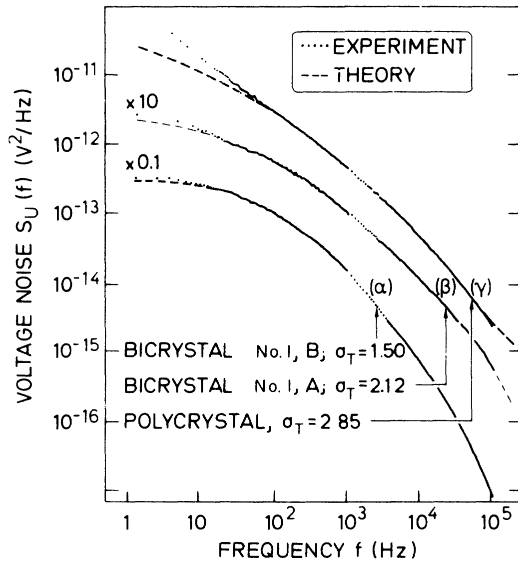

FIG. 11. Figure illustrates how transition from Lorentzian noise to $1/f$ noise occurs by the increasing strength of potential fluctuations. The bicrystal boundaries (curves α,β) show $1/f$ behavior over 1–2 frequency decades. Curve from the polycrystal with $\sigma=2.85$ displays $1/f$ noise over about 3 decades.

values of the parameter σ_T. With increasing spatial disorder, i.e., increasing σ_T, an increasing range of time constants τ contributes to the noise spectrum $S_U^{PF}(f)$. Equation (34) gives us thus an explicit relation between the degree of spatial disorder at the grain boundary and the range of time constants which are relevant for the fluctuation phenomena in such a disordered system.

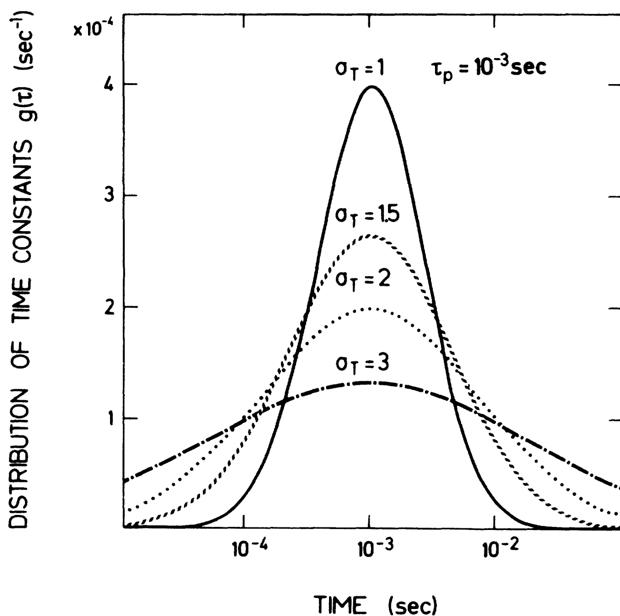

FIG. 12. Spatial potential fluctuations with a normalized standard deviation σ_T result in a spatial distribution $g(\tau)$ of time constants for trapping processes. Figure shows $g(\tau)$ according to Eq. (34) for different σ_T with a mean capture time constant τ_P.

The particular junction grain boundary is a model system to investigate quantitatively the various stages of the transition from Lorentzian to $1/f$ noise which is caused by the increasing disorder at the interface. An explicit expression—as given in Eq. (34)—exists for the distribution of time constants that describes this transition. We consider therefore *spatial* disorder as a possible mechanism for the general occurence of $(1/f)$-like noise in physical systems.

X. CONCLUSIONS

We propose a new model for the explanation of electrical fluctuation phenomena in the current flow across semiconductor grain boundaries. On the one hand, this model takes properly into account the trapping processes at the interface which modulate the thermionic current via the control of interface charge and band bending. The resultant amplification—described in our trap-transistor model—leads to considerable noise in the measured voltage drop across the barrier. Hence, interface properties are easily accessible to noise experiments. On the other hand, our model explicitly accounts for spatial inhomogeneities within the boundary plane. The localization of carriers results in considerable spatial potential fluctuations. The potential fluctuations yield a distribution of time constants with the consequence of a transition from Lorentzian to $(1/f)$-like noise.

Our combined model of trap-transistor action and potential fluctuations allows us to use noise measurements as a spectroscopic tool of grain boundary interface states. As a result we obtain the density of interface states N_{SS}, the capture cross section S_p, and the standard deviation σ of spatial potential fluctuations. The density of states N_{SS} reveals a continuous energy distribution and tail states near the band edges. The experimental finding of band tailing which is a consequence of disordered bonds[26] corroborates our model that is based on the assumption of spatial inhomogeneities. The voltage dependence of the capture cross section S_p can be interpreted in terms of a dependence of the capture probability on the velocity of carriers which cross the interface. The standard deviation σ of the spatial potential fluctuations can be related to the correlation length λ of the spatial charge distribution.

By extending our analysis to coarse-grained multicrystalline samples, we are able to give a quantitative explanation for the noise of this material. The potential fluctuations model naturally accounts for the different heights of the potential barriers in the polycrystal. Hence, noise measurements yield useful information on the electronic properties of bicrystal boundaries as well as on boundaries in coarse-grained multicrystals; results of noise from fine-grained films for very-large-scale integration technology applications were previously reported.[32]

The present paper has shown that a common prejudice against noise measurements can be overcome: The seemingly lack of structure in the frequency dependence of noise which often approaches $1/f$ behavior prevented

often thus far the use of noise experiments as a quantitative analysis tool. We have here demonstrated that a high experimental resolution of the noise data reveals deviations from pure $1/f$ noise. A precise analysis of the overall frequency dependence yields important information about physical parameters of the system under investigation. Our quantitative model furnishes the foundation for the use of noise measurements as a spectroscopic tool for electronic defects at semiconductor grain boundaries.

ACKNOWLEDGMENTS

We thank Hermann Stoll from the Max-Planck-Institut für Metallforschung, for much expert technical advice and valuable comments. We appreciate the continuous encouragement and support of Hans-Joachim Queisser. Thanks are due to Joachim Trost for his help with the computer programs and due to Lars Tilly, University of Lund, for his support during the measurements. Yincheng Lu provided us with some excellent bicrystals.

[1]F. N. Hooge, T. G. M. Kleinpenning, and L. K. J. Vandaume, Rep. Prog. Phys. **44**, 479 (1981).

[2]P. H. Handel, Phys. Rev. A **22**, 745 (1980).

[3]L. B. Kiss and P. Heszler, J. Phys. C **19**, L631 (1986), and references therein.

[4]A. L. McWhorter, in *Semiconductor Surface Physics,* edited by R. H. Kingston (University of Pennsylvania Press, Philadelphia, 1957), p. 207.

[5]K. S. Ralls, W. J. Skocpol, L. D. Jackel, R. E. Howard, L. A. Fetter, R. W. Epworth, and D. M. Tennant, Phys. Rev. Lett. **52**, 228 (1984).

[6]E. H. Nicollian and A. Goetzberger, Bell Syst. Tech. J. **46**, 1055 (1967).

[7]E. H. Nicollian and H. Melchior, Bell Syst. Tech. J. **46**, 2019 (1967).

[8]J. Werner, in *Polycrystalline Semiconductors,* edited by G. Harbeke (Springer, Berlin, 1985), p. 76.

[9]A. J. Madenach and J. Werner, Phys. Rev. Lett. **55**, 1212 (1985).

[10]H. J. Queisser, Mater. Res. Soc. Proc. **14**, 323 (1983).

[11]D. J. Bartelink, Mater. Res. Soc. Proc. **5**, 249 (1982).

[12]B. Authier, in *Festkörperprobleme XVIII,* edited by J. Treusch (Vieweg, Braunschweig, 1978), p. 1.

[13]Y. C. Lu, J. Cryst. Growth **79**, 322 (1986).

[14]M. M. Mandurah, K. C. Saraswat, and C. R. Helms, J. Appl. Phys. **51**, 5755 (1980).

[15]G. E. Pike and C. H. Seager, J. Appl. Phys. **50**, 3414 (1979).

[16]W. Shockley and J. R. Read, Phys. Rev. **87**, 835 (1952); R. N. Hall, *ibid.* **86**, 600 (1952).

[17]H. Haken, *Synergetics* (Springer, Berlin, 1983), pp. 147–149.

[18]C. W. Gardiner, *Handbook of Stochastic Methods* (Springer, Berlin, 1983), pp. 16 and 17; A. van der Ziel, *Noise: Sources, Characterization, Measurement* (Prentice Hall, Englewood Cliffs, 1970), p. 89.

[19]K. M. van Vliet and G. R. Fassett, in *Fluctuation Phenomena in Solids,* edited by R. E. Burgess (Academic, New York, 1965), p. 273, Eq. (13).

[20]K. Lee, K. Amberiadis, and A. van der Ziel, Solid-State Electron. **25**, 999 (1982).

[21]J. Werner and H. Strunk, J. Phys. (Paris) Colloq. **43**, C1-89 (1982).

[22]J. J. Simonne, Solid-State Electron. **16**, 121 (1973).

[23]J. Werner, W. Jantsch, and H. J. Queisser, Solid State Commun. **42**, 415 (1982).

[24]J. M. Ziman, *Models of Disorder* (Cambridge University Press, Cambridge, 1979), Chap. 13.

[25]M. H. Cohen, H. Fritsche, and S. R. Ovshinsky, Phys. Rev. Lett. **22**, 1065 (1969).

[26]J. Werner and M. Peisl, Mater. Res. Soc. Proc. **46**, 575 (1985); Phys. Rev. B **31**, 6881 (1985).

[27]C. M. Soukoulis, M. H. Cohen, and E. N. Economu, Phys. Rev. Lett. **53**, 616 (1984).

[28]P. Bräunlich, in *Thermally Stimulated Relaxation in Solids,* edited by P. Bräunlich (Springer, Berlin, 1979), p. 1.

[29]E. H. Rhoderick, *Metal-Semiconductor Contacts* (Clarendon, Oxford, 1978), p. 84.

[30]A. Rose, *Concepts in Photoconductivity and Allied Problems* (Interscience, New York, 1963), Chap. 7.

[31]J. R. Brews, J. Appl. Phys. **43**, 2306 (1972).

[32]A. J. Madenach and H. Stoll, in *Proceedings of the Ninth International Conference of Noise in Physical Systems, Montréal, 1987,* edited by C. M. Van Vliet (World Scientific, Singapore, 1987), p. 74; A. J. Madenach and J. Werner, Phys. Rev. B **38**, 1958 (1988).

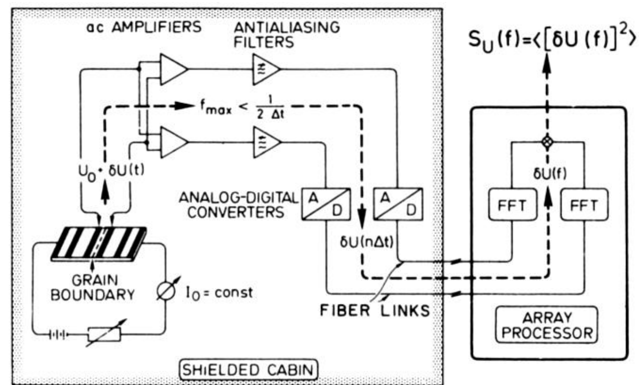

FIG. 1. Experimental setup and contact configuration for measurements at a bicrystal sample. Dashed line indicates how noise voltage $\delta U(t)$ is amplified, filtered, digitized, and transmitted via optical fiber links to the array processor. Signal is split into two branches to enable separate fast Fourier transformation (FFT) and cross correlation which averages out interfering amplifier noise. All devices in the shielded cabin are battery operated.

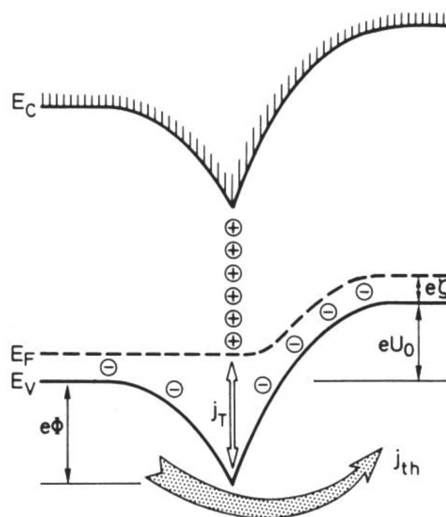

FIG. 3. One-dimensional band diagram at the grain boundary. Only donorlike interface states are drawn for simplicity. The positive interface charge is compensated by negative acceptor ions within the space-charge region. The application of a voltage U results in a thermally emitted current j_{th} over the barrier $e\Phi$. The current j_T represents the capture and emission of holes by the interface states.